Ahlul Bayt International University

Concepts and Functions in The Building Engineering

Journal homepage: https://cfbejournal.abu.ac.ir/

Investigation of the effect of velocity in the ogive projectile on the energy absorption mechanism and damage pattern in a three-layer reinforced concrete slab

Safa Peyman*; Seyyed Mehdi Mehdiyanzadeh DOI:
Professor, Department of Civil Engineering, Emame Hoseyn University, Tehran, Iran
Corresponding author: seyedmehranmh79@ihu.ac.ir

ARTICLE INFO

Article history:
Received: 15 September 2024
Revised: 26 October 2024
Accepted: 02 December 2024

Keywords:
Abaqus, reinforced concrete slab, numerical simulation, impact and penetration, projectile.

ABSTRACT

In this study, the impact resistance of multilayer reinforced-concrete slabs with compressive strengths of 30 MPa, 40 MPa and 140 MPa was investigated under the action of an oblong projectile impact using the Abaqus software. The slabs considered have overall dimensions of675×675 mm and a total thickness of 200 mm; each individual layer is 6.66 mm thick. The slabs were subjected to projectile impacts at velocities of 641 m /s and 541 m /s. The projectile mass is 0.386 kg, its length is 152 mm, its diameter is 3.25 mm, and it has a caliber-ratio head radius of 31 Based on the results, the optimal arrangement of the concrete layers from the highest to the lowest compressive strength (140 MPa – 41 MPa – 30 MPa) provides the greatest energy absorption and the lowest residual projectile velocity. This configuration achieves a performance close to that of a monolithic high-strength slab while using the material more efficiently, making it an economical option for protective structures. At lower impact velocities the slab mainly dissipates energy, but as the velocity increases the projectile tends to follow the path of least resistance rather than activating the slab's energy-absorption capacity. Consequently, failure occurs primarily by channel formation, clearly indicating that each reinforced-concrete slab possesses a threshold impact velocity above which the failure mode changes.

E-ISSN: 000-000

How to cite this article:
S. Peyman; S. M. Mehdiyanzadeh, (2024 Investigation of the effect of velocity in the ogive projectile on the energy absorption mechanism and damage pattern in a three-layer reinforced concrete slab (a.s.) International University, 1(2), 1-14. https://

Introduction

Reinforced concrete is one of the most widely used structural materials in the world due to its unique properties, including high strength, good durability, and environmental compatibility. Considering the increasing security threats such as terrorist attacks and the importance of designing structures resistant to penetration, investigating the behavior of structures against impact loads has become an inevitable necessity. Investigating the effect of bullet impact on the mechanical behavior of three-layer concrete with different strengths and arrangements will help improve the design of more resistant structures and can also help design and develop advanced concrete with better performance against high-energy impacts. Also, its application in military (such as bunker walls) or industrial (such as blast-resistant walls) structures can reduce economic costs and human casualties. Subsequently, numerous studies have investigated the behavior of reinforced concrete slabs against impact loads and projectile penetration. Jacobsen et al. [1] showed that the effect of reinforcement on increasing the strength of the slab is only evident in the case of direct projectile impact, and the compressive strength of concrete has a greater effect on ballistic resistance. In contrast, Shu et al. [2] emphasized the importance of impact velocity and concrete compressive strength in very thick slabs. Leu et al.[3], by numerically-experimental investigation of 80 mm reinforced concrete slabs, showed that the elastic modulus of concrete has a greater effect than the fracture toughness on the impact response and that the K&C model is an effective tool for impact analyses. Other studies have investigated various aspects of this issue. Wu et al. [4] presented a three-stage model for projectile penetration in concrete and investigated the effect of nose shape and concrete strength. Pavlovich et al. [5] compared the experimental and numerical results of projectile impact and confirmed the reliability of numerical simulation. Ren et al. [6] determined the parameters of the Holmquist-Johnson-Cook model for high-strength concrete and confirmed the accuracy of the model with experimental data. The effect of projectile shape and the use of lightweight concrete has also been considered. Osif et al. [7] showed that the shape of the projectile nose affects the penetration depth and failure mechanism in lightweight aerated concrete. Osif et al. [8] numerically investigated the behavior of reinforced and unreinforced concrete panels and confirmed the importance of reinforcement in increasing ballistic resistance. Also, Lee et al. [9] investigated the effect of rebar arrangement on the strength of concrete slabs and showed the effect of reducing the rebar spacing in improving the local strength of the slab. In the context of multilayer targets, Bisht and Iqbal [10] showed that increasing the number of layers with a constant overall thickness may reduce the strength and placing a thicker layer at the back performs better. Das and Nantagopalan [11] reviewed the role of fiber addition in increasing tensile strength and reducing penetration depth. Antonio et al. [12] compared the performance of common concrete behavior models and emphasized the importance of calibrating parameters based on laboratory data.

1- Steel and concrete behavior model

Johnson-Holmquist Destruction Behavioral Model (JH-2)

Several mechanistic models have been used to describe the dynamic behavior of brittle materials under impact loads. In this paper, the Johnson-Holmquist (JH-2) damage model is used to analyze the impact behavior of a reinforced concrete panel penetrated by a steel-tipped projectile. JH-2 is the second version of the Johnson-Holmquist (JH-1) ceramic model that is able to simulate the impact behavior of brittle materials, such as expansion, stress-strain dependence, and strain rate effects due to damage. According to the JH-2 model, the yield strength is degraded by damage accumulation, while in the JH-1 model, the yield strength is degraded only when a critical amount of damage is reached. The strength is defined in terms of equivalent stress as follows:

$\sigma*=\sigma i*-D(\sigma i*-\sigma f)$

where σ_i^* is the normalized equivalent stress in the intact, D is the damage variable, and the normalized equivalent stress at failure. It should be noted that intact and fully damaged materials are represented by damage values D=0 and D=1, respectively. The strength equations can also be defined in general form by normalizing the equation terms.

The equivalent stress at the elastic limit (HUGONOT) (HEL) is related to a one-dimensional shock wave exceeding the elastic limit as follows.

$$\sigma_{HEL} = \frac{3}{2}(HEL - P_{HEL})$$

where P_{HEL} is the pressure in HEL. After normalization, equation (3) can be rewritten as

$$\sigma* = \frac{\sigma}{\sigma_{HEL}}$$

According to the JH-2 model, it is assumed that the strength equation in intact and fully damaged material states can be expressed as a function of pressure and strain rate, respectively, as follows:

$$\sigma_i^* = A(P^* + T^*)^N(1 + C ln\varepsilon^*) \leq \sigma_i^{max}$$

$$\sigma_f^* = B(P^*)^M(1 + C ln\varepsilon^*) \leq \sigma_f^{max}$$

where the material components are A, B, C, M, and N and limits the strengths σ_i^{max} and σ_f^{max}.

The normalized stress is defined as:

$$P^* = \frac{P}{P_{HEL}}$$

where P is the actual pressure. The normalized maximum tensile hydrostatic pressure is also written as.

$$T^* = \frac{T}{T_{HEL}}$$

where T is the maximum tensile stress tolerated by the material. The JH-2 model uses damage accumulation similar to the Johnson-Cook model and assumes that damage increases with plastic strain as follows.

$$D = \sum \frac{\Delta \bar{\varepsilon}^{pl}}{\bar{\varepsilon}^{pl}(P)}$$

$$\bar{\varepsilon}^{pl} = D_1 (P^* + T^*)^{D_2}; \bar{\varepsilon}_{fmin}^{pl} \le \bar{\varepsilon}^{pl} \le \bar{\varepsilon}_{fmax}^{pl}$$

It should be noted that $\bar{\Delta}^{pl}$ is the equivalent plastic strain increase and $(P)\bar{\varepsilon}_f^{pl}$ is the equivalent plastic strain at failure. In addition, D_1 and D_2 are constants. The components $\bar{\varepsilon}_{fmin}^{pl}$ and $\bar{\varepsilon}_{max}^{pl}$ are introduced to limit the minimum and maximum values of the failure strain. The pressure-volume relationship of a brittle material is defined as:

$$P = \begin{cases} K_1\mu + K_2\mu^2 + K^3\mu_3 & if\mu \ge 0\ (compression) \\ K_3 & if\mu \le 0\ (tension) \end{cases}$$

where K1, K2, k3 are material constants, $\mu = {}^{\rho}/_{\rho_.} - 1$ where ρ and $\rho_.$ represent the current and reference density, respectively. When a material ruptures, an additional pressure increase ΔP is added, which takes the following expression:

$$P = K^1\mu + k_2\mu^2 + k_3\mu^3 + \Delta P$$

The determination of the stress increase is determined based on the energy considered. When the material is damaged, the elastic energy of the deflection ΔU decreases due to the decrease in strength. **Figure** shows the stress-volume strain relationship according to the JH-2 model.

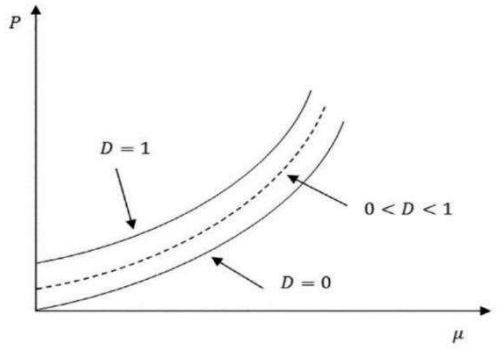

Figure 1. Stress-strain relationship of JH-2 model

The decrease in elastic energy is converted into potential energy through the increase in pressure ΔP, so that

$$\Delta P_{t+\Delta t} = -K_1\mu_{t+\Delta t} + \sqrt{(K_1\mu_{t+\Delta t} + \Delta P_t)^2 + 2\beta K_1 \Delta U}$$

where β is the fraction of the increase in elastic energy converted to potential energy. ($0 \le \beta \le 1$)

In the simulations performed, the properties of the concrete used were considered according to Table 1.

Table 1. Johnson-Helmquist model parameters for concrete SI [8, 10, 12]

Symbol	$f_c = 140$	$f_c = 140$	$f_c = 140$
$P\ kg/m^3$	۲۶۰۰	۲۴۴۰	۲۴۰۰
$G\ (GPa)$	۲۶.۷۷	۱۴.۸۶	۱۲.۵
ν	۰.۱۵	۰.۱۵	۰.۱۵
A	۱.۴۱	۰.۳	۰.۶۳۰۴
B	۰/۷۹	۲	۰.۲۱۰۱
n	۰.۷۷	۰.۷۵	۰.۸۴۳۷
C	۰.۱۱۸	۰.۰۰۷	۰.۰۰۶
m	۰.۶۱	۰.۶۱	۰.۸۴۳۷
$\dot{\varepsilon}_.$	۰	۱	۰
S_{max}	۷	۷	۷
$T(GPa)$	۰.۰۰۴	۰.۰۰۴	۰.۰۰۳۴
$\bar{\varepsilon}^{pl}_{f,min}$	۰.۰۱	۰.۰۰۱	۰.۰۱
$\bar{\varepsilon}^{pl}_{f,max}$	۱	۱	۱
$P_{HEL}(MPa)$	۲۵۰	۳۳/۴۳	۸۱۱
$D_۱$	۰.۰۷۳	۰.۰۴	۰.۶
$D_۲$	۱	۱	۱
$K_۱\ (GPa)$	۲۲.۷	۱۷.۱۲	۱۶.۶۶۷
$K_۲\ (GPa)$	۱۷۱	−۱۷۱	۷۳/۱۹
$K_۳\ (GPa)$	۲۰۸	۲۰۸	−۲۳۶
$HEL(MPa)$	۵۱۰	۷۱.۱۲	۱۴.۸۱

1.2. Johnson-Cook Behavioral Model

Another behavioral model for defining the behavior of steel in Abaqus is the Johnson-Cook behavioral model. Two researchers named Johnson and Cook in 1982, using the experiments that Hancock and Mackenzie had conducted on various metals, presented an empirical relationship to express the combined effect of temperature and strain rate, which is widely used in numerical calculations. In this model, the stress is equivalent to the implicit function of the average plastic strain, temperature and strain rate based on the relationship.

$$\sigma = (A^{'} + B^{'}.\bar{\varepsilon}_p^n)\left(1 + C^{'}.ln\frac{\dot{\bar{\varepsilon}}_p}{\dot{\varepsilon_o}}\right)(1 - T^*)^m$$

In the above relationship, σ is the yield stress, $\bar{\varepsilon}_p^n$ is the effective (or equivalent) plastic strain, $\dot{\bar{\varepsilon}_p}$ is the effective (or equivalent) plastic strain rate, $\dot{\varepsilon_o}$ is the reference plastic strain rate. This equation has five experimental parameters n, C, B, A and m which are called material constants and T^* is the dimensionless temperature which is expressed by the relationship:

$$T^* = \frac{(T - T_{ref})}{(T_{melt} - T_{ref})}$$

Where T_{ref} is the ambient temperature and T_{melt} is the melting temperature of the material in question. The effective plastic strain is given by:

$$\bar{\varepsilon}_p = \int_0^t d\bar{\varepsilon}^p$$

where $d\bar{\varepsilon}^p$ is the effective plastic strain, which can be calculated from the plastic strain tensor $d\bar{\varepsilon}_{ij}$ In the simulations, the properties of the concrete used are considered according to the table. In the simulations, the properties of the steel used are considered according to Table 2.

Table 2. Johnson-Cook model parameters for steel SI [۸]

Parameter	value	Parameter	value
E (Pa)	2×10^{11}	d_1	-0.0705
ν $(\frac{kg}{m^3})$	0.33	d_2	1.732
ρ (Gpa)	7850	d_3	-0.54
A (MPa)	490	d_4	-0.54
B (MPa)	807	d_5	-0.015
N	0.73	θ_{melt} (K)	1800
M	0.94	θ_{trans} (K)	293

2. Numerical simulation and validation of results

To validate the results, the study of Wu et al. [13], which experimentally investigated the impact behavior of a reinforced concrete panel, was used. In this study, a reference model was simulated in the finite element software Abaqus/Explicit to verify the numerical modeling of concrete slabs under high-velocity impact loading. The reference concrete slab with a compressive strength of 41 MPa was defined under the Johnson-Helmquist (JH-2) behavioral model, and its material specifications are presented in Table 1. This slab has geometric dimensions of 675×675 mm and a thickness of 200 mm, and its boundary conditions are considered as four-sided clamped. For modeling the concrete section, 3D eight-node volumetric elements with reduced integration (C3D8R) were used. The meshing strategy aimed at increasing the accuracy in the critical area (projectile impact location) includes the use of fine and dense meshes with dimensions of 5 × 5 × 5 mm in this area and coarser meshes with dimensions of 10 × 10 × 10 mm in other areas of the slab. The reinforcing bars are also modeled with the Johnson-Cook behavioral model, the specifications of which are given in Table 2, and using three-dimensional truss elements of the period (T3D2). These reinforcements are embedded in three layers with a diameter of 6 mm along the length and width of the slab (8 in each direction) and with a grid arrangement. The meshing of the reinforcements is also done with a size of 2.5 mm. The loading by a projectile with an ogee tip is simulated; This projectile, which is modeled as a rigid body, has a mass of 0.386 kg, a length of 152 mm, and a caliber diameter of 25.3 mm with a caliber-to-head radius ratio of 31. The projectile was launched towards the slab with initial velocities between 540 and 730 m/s, and its mesh was assumed to be tetrahedral with a size of 2.5 mm.

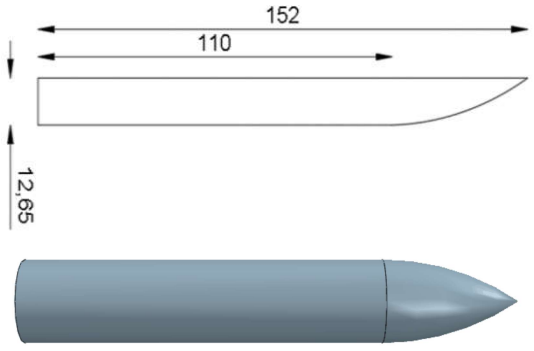

Figure 1. Geometry and characteristics of the Ogio projectile

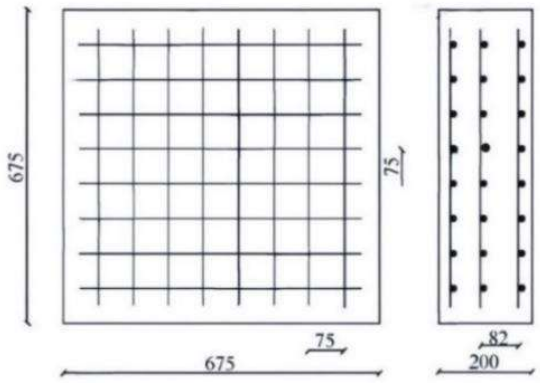

Figure 3. Concrete slab geometry and specifications

To assess the accuracy of the prediction of the damage pattern in the numerical model, the equivalent diameter of the damaged area was used as a comparison criterion, which is described below. Calculation of damage dimensions: The diameter dimensions of the pits created on the front and back surfaces of reinforced concrete slabs due to the penetration of the hard projectile were calculated. To calculate the equivalent diameter of damage D_M, D_1 , D_2 , D_3 and D_4 are required, which are shown in Figure 3 - Geometry and specifications of the concrete slab, and to calculate the diameter of the damage on the front and back surfaces of the pits, the equation shown below was calculated:

$$D_m = \frac{D_1 + D_2 + D_3 + D_4}{4} \quad (16)$$

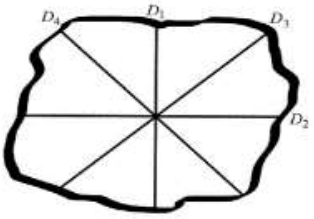

Figure 2. D_1, D_2, D_3 and D_4 are the diameters of the pit to calculate the equivalent diameter D_M

To investigate the numerical accuracy of the model in predicting the dynamic behavior of the projectile, the residual velocity value after passing through the slab was compared between the numerical analysis and experimental data at four different projectile velocities including 540, 597, 641 and 730 m/s. The extracted results, shown in Figure 5, the numerical model has a good agreement with the experimental data and indicate the validity and high accuracy of the model in representing the penetration process and analyzing the impact energy. The comparison of the pitting and delamination damages in numerical and experimental studies for the reinforced concrete slab under the impact velocity of 641 m/s is shown in Figure 6. The equivalent diameters on the front surface were obtained in the experimental and numerical studies as 275 mm and 277 mm, respectively, while on the back surface they were 241 mm and 276 mm, respectively. The difference between the results for the front surface was calculated to be 0.72% and for the back surface to be 15%.

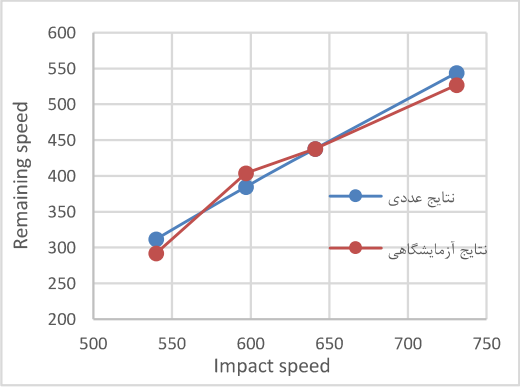

Figure 3. Comparison of residual velocity after collision in numerical and laboratory studies

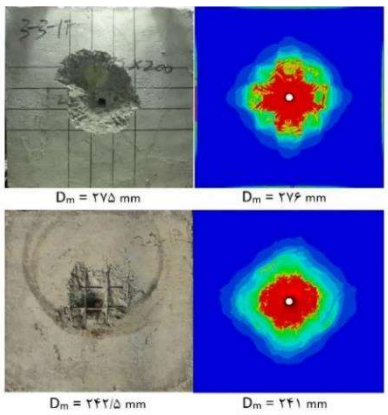

Figure 6. Slab damage in modeling and laboratory model

3. Numerical modeling and analysis of results

3.1. Numerical modeling of three-layer slab

In the continuation of the validation process, the numerical models proposed in this study were developed by maintaining the same geometry, boundary conditions, and reinforcement method as the validation model in order to examine the effect of changing the desired parameters separately. For this purpose, the dimensions of the slabs (675 mm in length and width and 200 mm in thickness), the type of supports (four-way bracing), the method of reinforcement (two-dimensional grid including 8 bars in each direction with a diameter of 6 mm), and the size of the grid elements in critical areas (5 mm) and other areas (10 mm) were considered as in the validation model. In the steel materials section, the same Johnson-Cook behavioral model with the parameters provided in the validation stage was used to maintain the integrity of the model and only the changes related to concrete and projectile shape were considered as the main variables. The main difference between the models of the present study and the validation is in the concrete section of the slab and the projectile velocity (540 and 641 m/s). In these models, the slab consists of three concrete layers with equal thickness (6.66 mm) and different compressive strengths (30, 41, and 140 MPa). The mechanical properties of each layer were determined based on the parameters of the JH-2 model, and the values of the concretes of 30, 41, and 140 MPa were selected according to the data in Table 1.

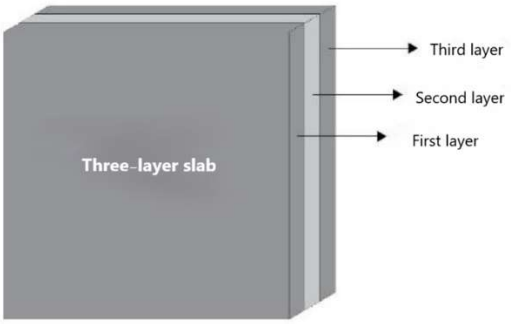

Figure 4 - Overview of three-layer slabs

3.2.Data analysis

3.2.1.Changes from kinetic to internal energy

In this section, in order to better understand the dynamic behavior of three-layer reinforced concrete slabs against projectile impacts with speeds of 540 and 641 m/h, the results of numerical simulations were analyzed and reviewed. The analyses were designed to examine the impact of key factors on the response of the structure. Figures 8 to 13 show the graphs related to the changes in kinetic energy of the projectile to the internal energy of the reinforced concrete slab. The samples were grouped purposefully. In this method, two samples that shared the strength of the first layer were selected. Then, the energy changes of these two samples were compared with three baseline control samples.

Figure 8 - Internal energy and kinetic energy diagram at a speed of 540 m/s

Figure 9 - Internal energy and kinetic energy diagram at a speed of 540 m/s

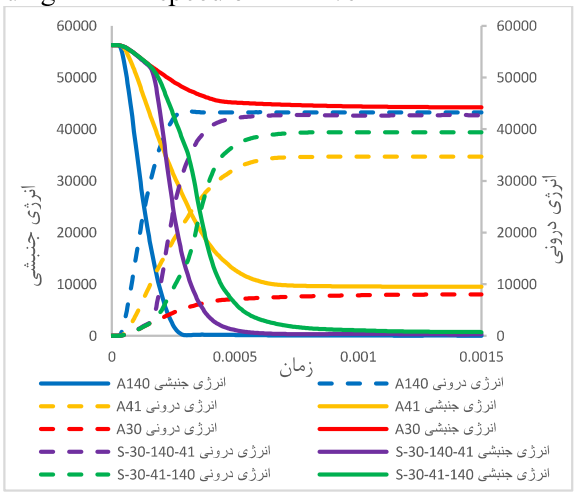

Figure 10 - Internal energy and kinetic energy diagram at a speed of 540 m/s

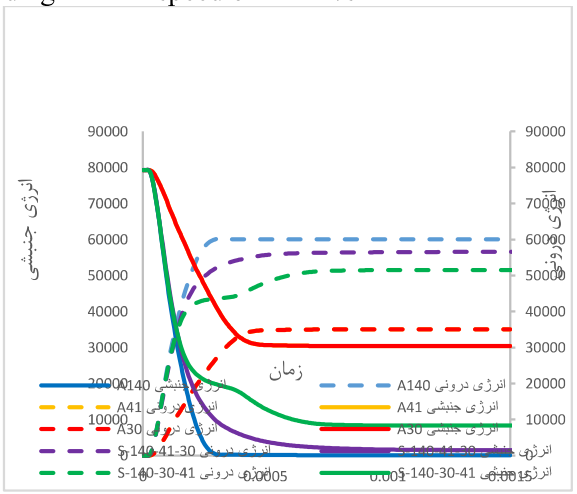

Figure 11 - Internal energy and kinetic energy diagram at a speed of 641 m/s

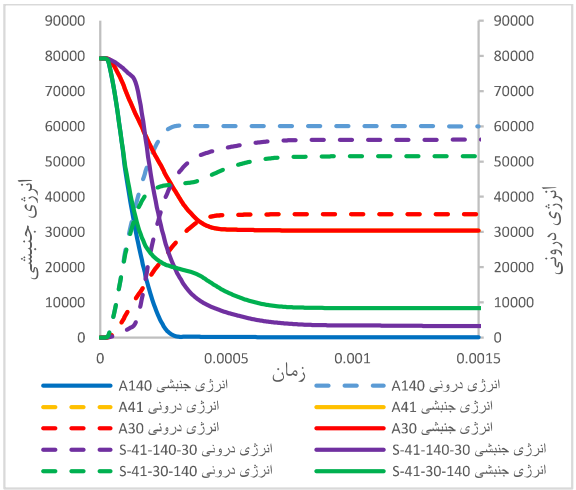

Figure 12 -Internal energy and kinetic energy diagram at a speed of 641 m/s

Figure 13 – Internal energy and kinetic energy diagram at a speed of 641 m/s

At 540 m/s, the slab is mainly capable of absorbing energy through extensive elastic and plastic deformation mechanisms and the stress concentration is well managed; as a result, the penetration depth is minimal and the damage remains mainly shear or compressive in the contact layer. However, as the velocity reaches 641 m/s, the nature of the phenomenon changes. At this high velocity, the kinetic energy of the projectile reaches a level where the resistance of the concrete to shear and compressive stresses exceeds its tensile and penetration strengths. As a result, instead of activating the energy absorption capacity of the structure, the projectile chooses the pure penetration path of least resistance and the destruction occurs mainly in the form of channel generation. This observation clearly shows that there is a threshold velocity for any geometric configuration of the projectile and slab; whenever this threshold is exceeded, the dominant mechanism shifts from controlled energy absorption to destructive penetration, and the effectiveness of design measures (such as concrete layering) is greatly reduced.

3.2.2. Analysis of the relationship between the volume of destruction and the residual velocity of the projectile

Evaluating the performance of a structure against severe dynamic loadings such as projectile impact requires the simultaneous examination of three key indicators: volume, penetration depth damage, and residual velocity of the projectile. These three criteria indicate how energy is distributed and absorbed. Therefore, simultaneous analysis of these three indicators can reveal the actual performance of the structure. Accordingly, four main states can be defined:

- First state: low damage + zero residual velocity → optimal and resistant performance (effective energy distribution).
- Second state: high damage + zero residual velocity → optimal performance in terms of energy absorption (sacrificing behavior).
- Third state: high damage + high residual velocity → poor performance (extensive damage and projectile passage).
- Fourth state: low damage + high residual velocity → worst case (free passage of the projectile and complete inefficiency of the structure).

In order to qualitatively and quantitatively compare the performance of different models, a relative scoring system was used. The best performance for the control sample A140 received a score of 100 and the worst performance for the control sample A30 received a score of 0. Other conditions were also scored as a linear minefield between these two limits, depending on how close they were to the desired or undesirable conditions.

economic efficiency of the proposed optimization approach in practical applications.

Table 2 - Table of four functional states and scoring of samples

Score	Mode	Percentage of destruction	Penetration depth (cm)	Residual velocity of the projectile	Initial speed	Sample names
88.47	2	19.5	passed	43.34	540	S-30-41-140-O-540
85.38	2	23.1	15.23	60.12	540	S-30-140-41-O-540
84.87	2	27.2	passed	52.69	540	S-41-30-140-O-540
93.33	2	19.6	13.33	27.79	540	S-41-140-30-O-540
96.58	2	21.1	17.14	7	540	S-140-30-41-O-540
100	2	20.4	8.6	0	540	S-140-41-30-O-540
99.89	1	17.4	5.8	6.33	540	A140-O-540
52.6	4	14.0	passed	219.2	540	A41-O-540
0	4	8.6	passed	474.5	540	A31-O-540

Score	Mode	Percentage of destruction	Penetration depth (cm)	Residual velocity of the projectile	Initial speed	Sample names
34.65	3	27.2	passed	241.6	641	S-30-41-140-O-641
56.04	2	24.0	passed	158.8	641	S-30-140-41-O-641
44.39	3	24.8	passed	204.8	641	S-41-30-140-O-641
64.58	2	28.3	passed	120.2	641	S-41-140-30-O-641
42.91	3	30.8	passed	204.8	641	S-140-30-41-O-641
75.6	1	22.3	passed	82	641	S-140-41-30-O-641
100	1	18.7	8.57	0	641	A140-O-641
0	4	13.7	passed	394.3	641	A41-O-641
0	4	13.7	passed	394.3	641	A31-O-641

4. Conclusion

The investigations showed that the sequence of compressive strength layers has a crucial influence on the dynamic performance of three-layer slabs. It was found that the optimal arrangement, in which the layers are arranged in an ascending order from low strength (30 MPa) to high strength (140 MPa) from the impact surface to the depth, provides the highest energy absorption and the greatest reduction in projectile velocity. This structural optimization ensures that the initial impact energy is dissipated in the surface layer, preventing deep penetration and damage propagation. In contrast, the reverse arrangement (140 → 30 MPa) resulted in the lowest energy absorption, because the projectile, with little loss in the upper layers, inflicts greater damage on the harder back layer. This finding emphasizes that the resistance gradient in the direction of projectile motion is a decisive parameter in the design of impact-resistant structures. The analysis of the effect of impact velocity on slab performance provides clear confirmation of the importance of kinetic energy in the penetration process. As expected, the increase in impact velocity from 540 m/s to 641 m/s was directly associated with an exponential increase in the damage rate and penetration depth. This dependence indicates that at lower velocities (e.g. 540 m/s), the slab is mainly capable of absorbing energy through extensive elastic and plastic deformation mechanisms and stress concentration is well managed; as a result, the penetration depth is minimal and the damage remains mainly in the form of shear or compression in the contact layer. With increasing velocity, the projectile chooses the net penetration path of least resistance instead of activating the energy absorption capacity of the structure and the damage occurs mainly in the form of channel generation. This observation clearly shows that there is a threshold velocity for any geometric configuration of the projectile and slab; whenever the velocity exceeds this threshold, the dominant mechanism shifts from controlled energy absorption to destructive penetration and the effectiveness of design measures (such as concrete layering) is severely reduced.

References

1. Ø. E. Jacobsen, M. Kristoffersen, S. Dey, and T. Børvik, "Projectile impact on plain and reinforced concrete slabs," *Journal of Dynamic Behavior of Materials,* vol. 10, no. 2, pp. 137-159, 2024.

[۲] X. Xu, T. Ma, and J. Ning, "Failure mechanism of reinforced concrete subjected to projectile impact loading," *Engineering Failure Analysis,* vol. 96, pp. 468-483, 2019/02/01/ 2019, doi: https://doi.org/10.1016/j.engfailanal.2018.11.006.

[٣] J. Liu, Z. He, P. Liu, J. Wei, J. Li, and C. Wu, "High-velocity projectile impact resistance of reinforced concrete slabs with ultra-high performance concrete strengthening-A numerical study," in *Structures*, 2023, vol. 52: Elsevier, pp. 422-436 .

[ٴ] H. Wu, Q. Fang, Y. Peng, Z. M. Gong, and X. Z. Kong, "Hard projectile perforation on the monolithic and segmented RC panels with a rear steel liner," *International Journal of Impact Engineering,* vol. 76, pp. 232-250, 2015/02/01/ 2015, doi: https://doi.org/10.1016/j.ijimpeng.2014.10.010.

[٥] A. Pavlovic, C. Fragassa, and A. Disic, "Comparative numerical and experimental study of projectile impact on reinforced concrete," *Composites Part B: Engineering,* vol. 108, pp. 122-130, 2017/01/01/ 2017, doi: https://doi.org/10.1016/j.compositesb.2016.09.059.

[٦] G.-M. Ren, H. Wu, Q. Fang ,and X.-Z. Kong, "Parameters of Holmquist–Johnson–Cook model for high-strength concrete-like materials under projectile impact," *International Journal of Protective Structures,* vol. 8, no. 3, pp. 352-367, 2017, doi: 10.1177/2041419617721552.

[٧] C. Oucif and L. M. Mauludin, "Numerical modeling of high velocity impact applied to reinforced concrete panel," *Underground Space,* vol. 4, no. 1, pp. 1-9, 2019/03/01/ 2018, doi: https://doi.org/10.1016/j.undsp.2018.04.007.

[٨] C. Oucif, L. M. Mauludin, and F. Abed, "Ballistic behavior of plain and reinforced concrete slabs under high velocity impact," *Frontiers of Structural and Civil Engineering,* vol. 14, no. 2, pp. 299-310, 2020/04 2020, doi: 10.1007/s11709-019-0588-5.

[٩] S. Lee, C. Kim, Y. Yu, and J.-Y. Cho" ,Effect of Reinforcing Steel on the Impact Resistance of Reinforced Concrete Panel Subjected to Hard-Projectile Impact," *International Journal of Impact Engineering,* vol. 148, p. 103762, 2021/02/01/ 2021, doi: https://doi.org/10.1016/j.ijimpeng.2020.10376.٢

[١٠] B. M. Belyakov, S. V. Glushkov, and M. B. Belyakov, "Numerical Study of Single- and Multi-Layer Concrete Targets under Steel Projectile Impact," (in English), *Strength of Materials,* vol. 55, no. 6, pp. 839-846, 2023, doi: 10.3103/S0039232423060042.

[١١] N. Das and P. Nanthagopalan, "State-of-the-art review on ultra high performance concrete - Ballistic and blast perspective," *Cement and Concrete Composites,* vol. 127, p. 104383, 2022, doi: 10.1016/j.cemconcomp.2021.104383.

[١٢] P. Xu and S. Zuo, "Study on the JH-2 model parameters for metro shield cutting reinforced concrete pile," *Geotechnical and Geological Engineering,* vol. 39, no. 7, pp. 5267-5278, 2021.

[١٣] H. Wu, Q. M. Li, Z. Tu, and Q. Zhang, "Semi-theoretical analyses of the concrete plate perforated by a rigid projectile," *International Journal of Impact Engineering,* vol. 49, pp. 174-185, 2012, doi: 10.1016/j.ijimpeng.2011.11.003.